

Understanding the Effects of Pressure, Anharmonicity and Phonon Softening on the Superconducting Critical Temperature

Chandan Setty^{1,*}, Matteo Baggioli^{2,†}, and Alessio Zacccone^{3,4,‡}

¹Department of Physics, University of Florida, Gainesville, Florida, USA.

²Instituto de Fisica Teorica UAM/CSIC, c/Nicolas Cabrera 13-15, Universidad Autonoma de Madrid, Cantoblanco, 28049 Madrid, Spain.

³Department of Physics "A. Pontremoli", University of Milan, via Celoria 16, 20133 Milan, Italy.

⁴Cavendish Laboratory, University of Cambridge, JJ Thomson Avenue, CB30HE Cambridge, U.K.

^{*}e-mail: settychandan@gmail.com

^{*}e-mail: matteo.baggioli@uam.es

[†]e-mail: alessio.zacccone@unimi.it

ABSTRACT

Electron-phonon superconductors at high pressures have displayed the highest values of critical superconducting temperature T_c on record, now rapidly approaching room temperature. A variety of other superconducting materials have been investigated experimentally in recent years, unveiling a zoology of different T_c trends as a function of applied pressure P . In spite of the importance of high- P superconductivity in the quest for room-temperature superconductors, a mechanistic understanding of the effect of pressure and its complex interplay with phonon anharmonicity and superconductivity is missing, as numerical simulation studies can only bring system-specific phenomenological insights. Here we develop a theory of electron-phonon superconductivity under an applied pressure which fully takes into account the anharmonic decoherence of the optical phonons. The results are striking: generic trends of T_c with increasing P observed experimentally in both elemental and more complex superconductors can be recovered and explained in terms of coherence/incoherence properties of the boson glue provided by anharmonically damped optical phonons within the governing gap equation. In particular, T_c first increases, then goes through a peak and then decays upon further increasing the ratio Γ/ω_0 , where Γ is the optical phonon damping and ω_0 the optical phonon energy at zero pressure and momentum. In other words, T_c increases with Γ/ω_0 in a regime where phonons behave like well-defined quasiparticles, and decays with Γ/ω_0 in a regime of strong anharmonic damping where phonons are incoherent ("diffusons"). This framework is able to explain recent experimental observations of T_c as a function of pressure in complex materials (e.g. TIInTe_2), where T_c first decreases with pressure then goes through a minimum after which it rises with pressure again. In a second scenario, which is experimentally realized in certain strongly correlated metals (e.g. the cuprates), the phonon quasiparticles are not well defined anymore ($\Gamma \gg \omega_0$), the underlining physics becomes incoherent and the T_c dependence on pressure is completely reversed but still predicted by our theoretical model.

Introduction

When a crystal lattice is subjected to a (hydrostatic) pressure deformation, its phonon frequencies change in response to the change of volume, in a way which is controlled by the material's Grüneisen parameter, hence by the anharmonicity of the vibration modes. However, the effects of these changes in the phonon frequencies, and of the related anharmonicity, on the superconducting properties of a material have largely remained poorly understood. Filling this knowledge gap is an urgent problem in order to develop an understanding of superconductivity in materials under pressure, which include the highest- T_c values recorded so far in the high-pressure hydride materials^{1–4}.

On one hand, a large number of experimental works have shown how the superconducting critical temperature T_c changes as a function of pressure P for a variety of materials. For elemental superconductors, a commonly observed trend in experiments is a decrease of T_c with increasing P , which has been theoretically predicted upon analyzing the behaviour of the Eliashberg electron-phonon coupling function $\alpha^2 g(\omega)$ as a function of P ^{5–9}. An increase of P typically shifts the $\alpha^2 g(\omega)$ distribution to higher frequencies, thus driving the system into an unfavourable regime¹⁰ for the electron-phonon coupling⁵. This behaviour is at odds with Ashcroft's famous expectation¹¹ that an increase of the Debye frequency ω_D would necessarily lead to an increase of T_c , which may hold for weak-coupling BCS materials, but not for strong-coupling materials with larger λ values. Also, a notable exception to the above standard rule for elemental superconductors is represented by α -uranium^{9,12}, to be

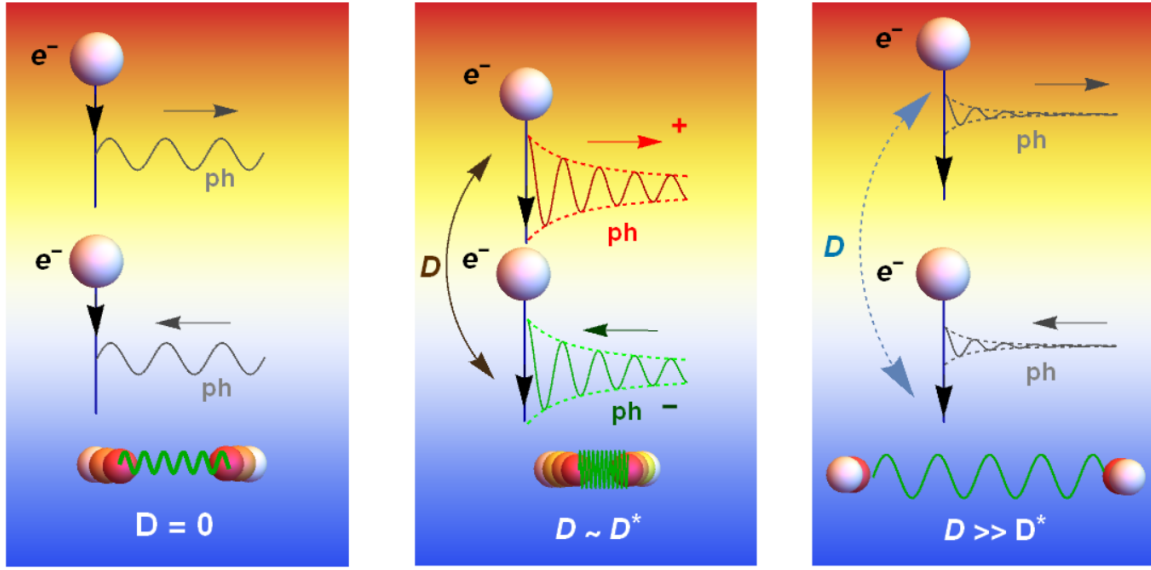


Figure 1. Mechanism of T_c enhancement through anharmonicity with two phonon modes. (**Left panel**) In the absence of anharmonic decoherence ($D = 0$), the Stokes (S-) and anti-Stokes (aS-) processes are insensitive to their phase and are thus indistinguishable. This scenario leads to ordinary Cooper pairing. (**Middle panel**) Weak anharmonic decoherence ($D \sim D^*$) sensitizes the phase of the S- and aS- processes and enables them to act coherently and enhance the effective coupling of electrons and phonons leading to strong Cooper pairs. (**Right panel**) For very strong anharmonicity ($D \gg D^*$), the S- and aS- processes are only weakly sensitive to their phases making them effectively indistinguishable while acting to reduce the effective coupling of electrons and phonons leading to weak pairing.

discussed in detail below, while another puzzling material such as bismuth is known to have a very low T_c at ambient pressure (on the order of the mK)^{13,14} and a decent T_c (7 – 8K) at higher pressures¹⁵. A similar surprising trend is observed upon introducing structural disorder into crystalline solids which may lead to the enhancement of T_c (as is the case for Bi and Be) in the amorphous state, an effect which has been recently explained in Ref.¹⁶ as due to the favourable effect of disorder-induced soft transverse phonon modes on the pairing.

Exploring the effect of P on more complex non-elemental materials has led to a zoology of trends of T_c as a function of P ¹⁷. On the other hand, numerical simulations have provided invaluable quantitative insights into the phonon dispersion relations, and into the structural stability of superconducting compounds, including many new materials. Numerical calculations also allow one to estimate the anharmonicity of the various phonon modes involved, by comparing fully anharmonic calculations with harmonic calculations^{4,18}. Despite these efforts, a mechanistic picture of high pressure effects on the superconducting state which takes into account anharmonic decoherence of the bosonic glue is missing.

As a matter of fact, early theoretical approaches^{5–9} ignored phonon anharmonicity while more recent works on the high- T_c hydrides^{18–29} only take into account the phonon energy renormalizations neglecting anharmonic decoherence. The latter is key to properly describe the effect of pressure on phonon-mediated Cooper pairing, as we will show in the following.

In this paper, we develop such theory by working with a gap equation derived from the Migdal-Eliashberg equations in the weak coupling BCS limit. Crucially, to mediate Cooper pairing, we implement optical phonon propagators which contain the effect of an external applied pressure and the resulting anharmonic decoherence via the optical phonon damping³⁰. The analytical theory is able to provide predictions that allow one to disentangle the complex interplay between pressure-induced changes of optical phonon energy and anharmonic decoherence, and their effects on the T_c .

Different physical regimes are predicted, which include (i) monotonic decrease of T_c with P ; (ii) non-monotonic trend with a minimum, in conjunction with optical phonon softening, which qualitatively explains recent experiments in TIInTe_2 ³¹; (iii) non-monotonic trend with a maximum in a regime of incoherent phonons where the quasi-particle picture breaks down.

Theoretical framework

Optical phonon energy under pressure

We start by analyzing the effect of external pressure on the optical phonons of a crystal lattice. The main effect of pressure is to induce a negative volume change of the material. The change of volume, in turn, is related to a change of phonon frequency, through the Grüneisen parameter, $\gamma = -d \ln \omega' / d \ln V$, via³²:

$$\frac{\omega'(V)}{\omega'_{P=0}} = \left(\frac{V}{V_0} \right)^{-\gamma}, \quad (1)$$

where $\omega'_{P=0}$ refers to optical phonon energy at zero ambient pressure. The above relations apply to individual phonon modes with frequency ω' .

The volume change is related to the change of pressure as described by the Birch-Murnaghan equation of state³³, which is derived based on nonlinear elasticity theory, and provides an expression for $P(V)$. Upon replacing V with ω' in (1), one obtains the following relation between the optical phonon frequency ω' and the applied pressure³²:

$$P(X) = \frac{3}{2} b_0 \left(X^7 - X^5 \right) \left[1 + \eta (1 - X^2) \right], \quad (2)$$

with $X \equiv (\omega' / \omega'_{P=0})^{\gamma/3}$. Upon inverting the above Eq.(2) to obtain ω' as a function of P , it is clear that ω' is a monotonically increasing function of P , with the increase being modulated by anharmonicity through γ . Also, $b_0 = B_0 / \gamma_0$, with B_0 the bulk modulus, while $\eta = (3/4)(4 - B'_0)$ with $B'_0 = dB_0/dP$.

In the above relations, the frequency ω' refers to the real part of the phonon dispersion relation, whereas the imaginary part of the dispersion relation is related to the phonon damping coefficient Γ (the inverse of the phonon lifetime), as follows

$$\omega^2 = \omega_0^2 - i\omega\Gamma + \mathcal{O}(q^2), \quad \omega' \equiv \text{Re}(\omega) = \frac{1}{2} \sqrt{4\omega_0^2 - \Gamma^2} + \mathcal{O}(q^2), \quad \frac{\Gamma}{2} \equiv \text{Im}(\omega) + \mathcal{O}(q^2). \quad (3)$$

Hence, ω' denotes the renormalized phonon energy measured e.g. in Raman scattering (i.e. the Raman shift), while Γ represents the linewidth of the Raman peak. Let us emphasize that these expressions are at leading order in the momentum q and higher order corrections $\mathcal{O}(q^2)$ are neglected at this stage.

We now introduce a key dimensionless parameter for the subsequent analysis

$$D \equiv \Gamma/\omega_0, \quad (4)$$

which quantifies the degree of coherence of the phonon. Low values of D signify high coherence of the phonons, which can thus be treated as approximately independent quasiparticles, whereas large D values correspond to incoherent vibrational excitations in the diffusive regime (“diffusons” in the language introduced by Phil Allen, Feldman and co-workers³⁴). The schematic picture that will emerge from the subsequent theoretical analysis is anticipated in Fig.1.

In the following section, we introduce the theoretical framework for the Cooper pairing and we will start by considering how the superconducting critical temperature T_c varies as a function of D .

Gap equation with anharmonic phonon damping

For a generic Fermionic Matsubara frequency ω_n and momentum \mathbf{k} , we denote the gap function as $\Delta(i\omega_m, \mathbf{k})$. With a constant coupling g , the gap equation can be derived from the Eliashberg equations in the one-loop (weak coupling) approximation, and takes the form^{35,36}

$$\Delta(i\omega_n, \mathbf{k}) = \frac{g^2}{\beta V} \sum_{\mathbf{q}, \omega_m} \frac{\Delta(i\omega_m, \mathbf{k} + \mathbf{q}) \Pi(\mathbf{q}, i\omega_n - i\omega_m)}{\omega_m^2 + \xi_{\mathbf{k} + \mathbf{q}}^2 + \Delta(i\omega_m, \mathbf{k} + \mathbf{q})^2}, \quad (5)$$

where β is the inverse temperature and V is the volume. In Matsubara frequency space, we choose the pairing mediator to be a damped optical phonon given by the bosonic propagator

$$\Pi(\mathbf{q}, i\Omega_n) = \frac{1}{\Omega(q)^2 + \Omega_n^2 + \Gamma(q)\Omega_n}, \quad (6)$$

where Ω_n is the bosonic Matsubara frequency, $\Omega(q) = \omega_0 + \alpha q^2$ is the phonon dispersion, and the damping factor, $\Gamma(q) \equiv D\omega_0$, is a constant independent of momentum for high-frequency optical phonons³⁰. In accordance with the Klemens formula³⁰,

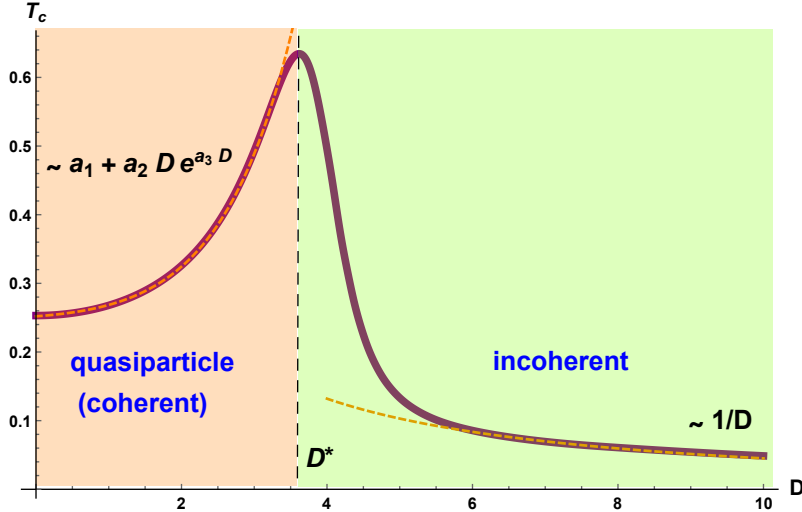


Figure 2. An illustration of the two regimes present in our model: the “coherent” regime where the critical temperature grows with $D \equiv \Gamma/\omega_0$ and the “incoherent” regime, where the functional dependence is inverted. In the “coherent” regime, the optical phonons behave like independent quasiparticles with frequencies renormalized by anharmonicity, whereas in the incoherent regime the quasiparticle coherence breaks down due to the large anharmonic damping.

one can also include an additional prefactor, $1 + \frac{2}{e^{\omega_0/2T} - 1}$, in the damping term $\Gamma(q)$ to account for a temperature dependent phonon linewidth. We find that this has a negligible effect on the results discussed below. The factor D controls the strength of the damping term and may change with pressure. The leading order contribution to the square of the dispersion is $\Omega(q)^2 \sim \omega_0^2 + vq^2$ where $v = 2\omega_0\alpha$. This is the first momentum correction which was neglected in Eq.(3). Assuming an isotropic, frequency-independent gap $\Delta(i\omega_n, \mathbf{k}) \equiv \Delta$, we can set the external frequency and momentum to zero without any loss of generality. Converting the resulting summation into an energy integral, the gap equation becomes

$$1 = \sum_{\omega_m} \int_{-\mu}^{\infty} \frac{\lambda T d\xi}{[\nu\xi + M^2 + \omega_m^2 - D\omega_m\omega_0][\omega_m^2 + \xi^2 + \Delta^2]}, \quad (7)$$

where $M^2 = \mu v + \omega_0^2$. Here we have defined the effective coupling constant $\lambda = N(0)g^2$, $N(0)$ is the density of states at the Fermi level, and μ is the chemical potential. We can now utilize the energy integral identity $\int_{-\infty}^{\infty} \frac{d\xi}{(z\xi + s)(\xi^2 + r^2)} = \frac{\pi s}{r(s^2 + z^2 r^2)}$ in the limit of large chemical potential to yield the gap equation

$$1 = \sum_{\omega_m} \frac{\lambda \pi T (M^2 + \omega_m^2 - D\omega_m\omega_0)}{\sqrt{\omega_m^2 + \Delta^2} [(M^2 + \omega_m^2 - D\omega_m\omega_0)^2 + (\omega_m^2 + \Delta^2)v^2]}. \quad (8)$$

We can now perform the final Matsubara sum after seeking a condition for T_c by setting $\Delta = 0$. Defining $p = \omega_0 D + iv$ and $Q_{\pm} = \frac{1}{2} (p \pm \sqrt{p^2 - 4M^2})$ leads to an equation for T_c that can be numerically solved given by

$$-M'^2 = \psi\left(\frac{1}{2}\right) + \frac{1}{4} \left[\left\{ \frac{p' - Q'_+}{Q'_+ - Q'_-} \psi\left(\frac{1}{2} - \frac{Q'_+}{2\pi T'_c}\right) + \frac{-p' + Q'_-}{Q'_+ - Q'_-} \psi\left(\frac{1}{2} - \frac{Q'_-}{2\pi T'_c}\right) + c.c \right\} + \{D \rightarrow -D\} \right], \quad (9)$$

where $\psi(x)$ is the digamma function, the primed quantities are dimensionless and are defined as $Q'_{\pm} \equiv \frac{Q_{\pm}}{\sqrt{\lambda}}$ and so on.

Results

Schematic T_c dependence on optical phonon energy and anharmonicity

Upon numerically solving Eq.(9) for a constant damping coefficient Γ , we can study the evolution of T_c as a function of the dimensionless parameter $D \equiv \Gamma/\omega_0$. The trend is shown in Fig.2. At low D values, T_c increases with D , then goes through a

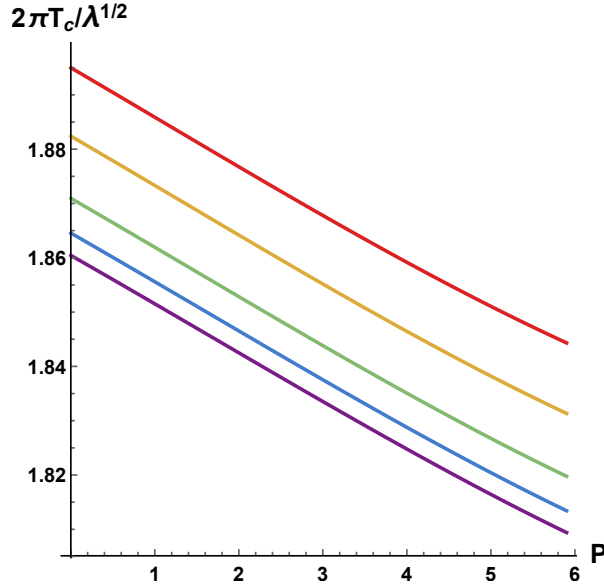


Figure 3. The normalized critical temperature with $D = \alpha\omega_0^4$ and ω_0 given by the formula Eq.(2). α increases from red to purple.

maximum after which it then decays sharply upon further increasing D . The maximum appears around $D^* \sim \mathcal{O}(1)$ with its exact value determined by the microscopic parameter M^2 . This corresponds exactly to the scale at which the real and the imaginary part of the phonon dispersion relation become comparable ($\Gamma \sim \omega_0$) and the phonons turn into quasi-localized “*diffusons*”. In this sense, this is analogous to the Ioffe-Regel crossover scale³⁷.

The mechanistic picture shown in Fig.1 can be used to understand the non-monotonic dependence of T_c upon the anharmonic decoherence parameter D . To begin, we note that in the absence of D , the gap equation in Eq. 7 has even terms only in the Matsubara frequency transfer ω_m . Hence both constructive Stokes (S-) and destructive anti-Stokes (aS-) processes, which emit and absorb energy respectively, contribute to the gap equation equivalently. However, when D is non-zero, Eq. 7 is sensitive to the sign of the energy transfer, thereby distinguishing the two processes. From this property, it is clear that the energy integral and Matsubara summations in Eqs. 7 and 8 lead to terms that are proportional to D in the numerator of the gap equation. Provided $D \lesssim D^*$, this effectively increases the electron-phonon coupling λ and hence the Cooper pair binding energy. For values of D much larger than D^* , the phonons are extremely damped and S- and aS- processes again contribute approximately equally to the gap equation, thus reducing the effective electron-phonon coupling.

At low values of damping Γ (low- D regime) and $\Gamma/\omega_0 \ll 1$, the real part of the dispersion relation dominates over the imaginary part, and the phonons behave like coherent quasiparticles with well-defined momentum k . In the opposite regime of large anharmonic damping $\Gamma/\omega_0 \gg 1$ (hence large D), we have that $\text{Im}\omega > \text{Re}\omega$, hence the phonons lose their coherence and the quasiparticle approximation breaks down. These two regimes correspond to two different Cooper pairing regimes. One regime we call the “coherent” regime (because here phonons behave like coherent quasiparticles), where T_c correlates positively with anharmonic damping (hence where damping enhances T_c). The second regime we call “incoherent” and here, instead, T_c decreases with further increasing the anharmonic damping. Notice that, in the coherent regime, T_c increases (decreases) as the optical phonon energy ω_0 decreases (increases), whereas the opposite trends apply in the incoherent regime. This implies that the effect of pressure can either promote or depress superconductivity depending on the underlying physics of the optical phonons in a given lattice.

The theoretical prediction in Fig.2 can be fitted with the following simple functions

$$T_c(D) \sim a_1 + a_2 D e^{a_3 D} \quad \text{for } D < D^* \text{ (coherent)}, \quad T_c(D) \sim D^{-1} \quad \text{for } D > D^* \text{ (incoherent)}, \quad (10)$$

with $a_n > 0$.

We will show below that these two regimes lead to radically different scenarios in terms of the dependence of T_c on the external pressure P . This conceptual schematization will be shown in the next sections to hold a number of consequences for a deeper mechanistic understanding of the effect of pressure on superconductivity in complex materials.

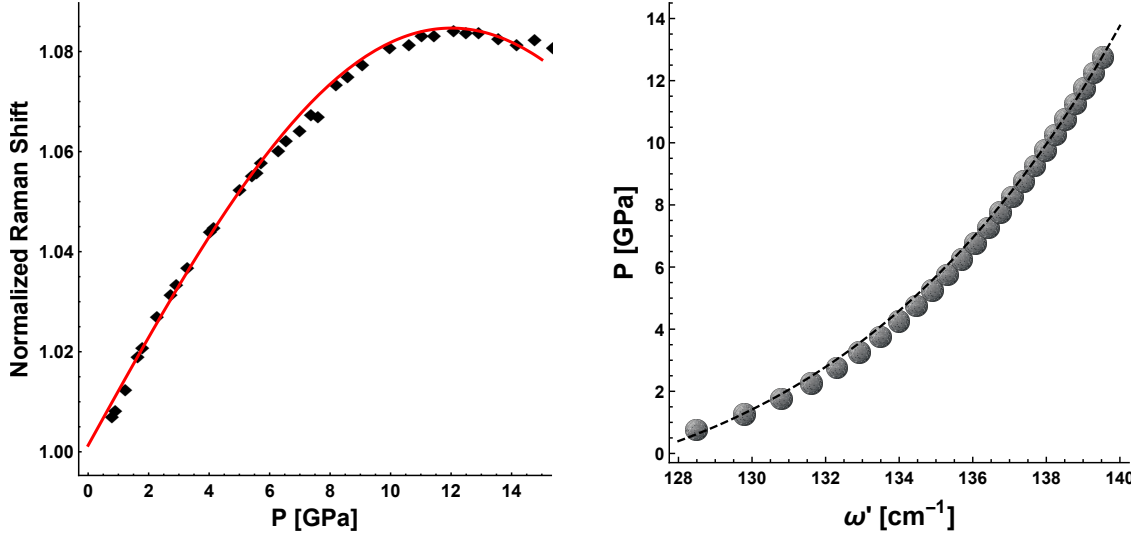


Figure 4. Left: The normalized Raman shift (proportional to ω') as a function of pressure and its fit with an empirical function. The value at zero pressure is $\approx 128 \text{ cm}^{-1}$. Data taken from³¹ **Right:** Comparison between the best empirical fit of³¹ (shown in the left panel) and the Eq. 2 in terms of $\omega_0 \approx \omega'$, ($\Gamma \ll \omega_0$). The parameters are set to the values shown in Eq.(11).

In Fig.2 we assumed that the pairing is mediated by high-frequency optical phonons near the Debye frequency ω_D for which the Klemens model gives a simplified (constant) anharmonic damping coefficient $\Gamma = D\omega_0$. In the more general case, the Klemens damping is given by $\Gamma = \alpha\omega_0^5$, where α is a prefactor which depends on the microscopic physics which governs the decay of the optical phonon into two acoustic phonons. Notably, $\alpha \sim \gamma^2$, where γ is the lattice Grüneisen parameter introduced above. The latter is a function of the interatomic potential³⁸, hence of the electronic orbital/bonding physics, and can be easily computed, for a given phonon mode in a give material, from first principles³⁹.

Using this more general Klemens formula for a generic optical phonon, we obtain the trends shown in Fig.3. A linear decreasing trend of T_c as a function of P is predicted by our theory for the coherent-phonon regime, in agreement with many experimental data sets in the literature for simple (e.g. elemental) superconductors^{9,17,40}.

Theoretical analysis of superconductivity in TIInTe_2 at high pressure

In this section, we explore the potential of the above framework to rationalize recent experimental data where highly non-trivial (e.g. non-monotonic) dependencies of T_c upon P have been observed, and for which a theoretical explanation is lacking. We study the paradigmatic case of TIInTe_2 , for which accurate experimental data are available for the optical phonon energy and the anharmonic damping, as measured by Raman scattering, and also for T_c , as a function of pressure.

We start by fitting the experimental data for the optical phonon energy (renormalized by anharmonicity) ω' as a function of pressure, displayed in Fig.4 left panel, by means of Eq.2, and we get:

$$b_0 = 8 \text{ GPa}, \quad \gamma = 5.8, \quad \eta = 0.05, \quad \omega'_{P=0} \approx \omega_{0,P=0} = 127 \text{ cm}^{-1}. \quad (11)$$

The fitting is shown in Fig.4 right panel, where the frequency values refer to ω' . The latter has been obtained by using Eq.3 in combination with Eq.2. The optical mode energy increases upon increasing P in a conventional way³² up to $P = 8 \text{ GPa}$, after which phonon softening, linked to the increase of anharmonic damping Γ is observed upon further increasing P , as shown in Fig. 4 left panel.

The increase of anharmonicity with pressure is clearly evidenced by the behaviour of the Raman peak linewidth Γ , as shown in Fig.5 left panel. Notice that the percentile growth of the linewidth under pressure is much larger than that of the normalized Raman shift. In this sense, the material is characterized by giant anharmonicities and the damping effects are fundamental. Here, in the same panel, different empirical trends are shown, alongside the experimental data which manifest a significant scatter. In general, $\Gamma \ll \omega_0$ for this system, such that this case belongs to the “coherent” regime discussed in the previous section and in Fig.2. Indeed, we checked that ω' and ω_0 differ by only about 0.01% at all P values. These different trends for Γ have been implemented, alongside the fitted optical phonon energy ω' from Fig.4, into our theoretical gap-equation framework for the prediction of T_c presented in the previous section of this paper. The resulting theoretical T_c trends are shown in Fig.5 in comparison with the experimental T_c data from Ref.³¹, as a function of the applied pressure.

All the Γ trends in Fig. 5 left panel clearly lead to the same qualitative dependence of T_c on P , with a minimum. The physics behind this trend is explained by our theoretical framework: at low P the T_c decreases because of the increase in P ,

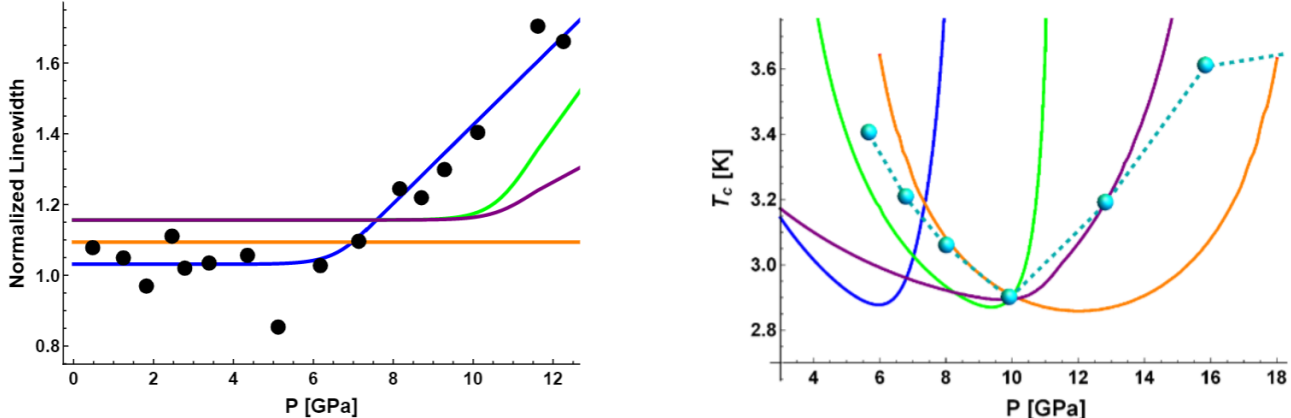


Figure 5. Left: The normalized linewidth and three different sets of fits. The zero pressure value is taken as 3.2 cm^{-1} . Data taken from³¹. **Right:** The corresponding theoretical calculations for the critical temperature (solid lines) are compared with the experimental data (symbols). The colors of the theoretical curves for T_c match the respective models for the linewidth in the left panel.

which induces an increase of the optical phonon frequency ω' or ω_0 . The subsequent phonon softening leads to the minimum and to an inversion of the trend: upon further increasing the pressure the T_c starts to rise. This is due to the fact that lower ω_0 values lead to a Stokes/anti-Stokes constructive interference (in the presence of anharmonic damping), which enhances the Cooper pairing,^{41,42}. This behaviour, with a minimum in T_c is independent of the particular Γ trend with P , and in fact occurs even for Γ constant with P .

The role of the Γ trend with P is to control the position of the minimum as a function of pressure. Also, importantly, the presence of a rise in Γ leads to a stronger rise after the minimum, which confirms that in the “coherent” regime the T_c can be strongly enhanced by the anharmonic damping, as discussed in the context of Fig.2. This finding has deep implications for high- T_c hydrogen-based materials, where the anharmonic damping of the optical phonons can be significant and may be tuned by the material design.

Positive pressure effect on T_c in the cuprates and other anomalous materials

Observation of T_c rising with the applied pressure P , i.e. $dT_c/dP > 0$, has been historically relatively rare, until the discovery of the high- T_c cuprates. Before the cuprates, not many materials displayed an enhancement of T_c with P , a notable case being that of α -uranium^{9,12}. Interestingly, α -uranium presents a vibrational density of states (VDOS) which is very rich of soft vibrational modes⁴³, traditionally attributed to anharmonicity in crystals⁴⁴, although their origin in α -uranium is still under debate⁴³. In general, the well known existence of phonon anomalies in α -uranium⁴⁵, suggests that it is highly possible that the observed rise in T_c with P (followed by a maximum) is due to incoherent vibrational excitations, which would support the scenario of the “incoherent” regime predicted by our theory in Fig.2.

Right after the discovery of the cuprates, a positive T_c vs P correlation has been observed in various high- T_c cuprate materials⁴⁶, including the first cuprate, the La-Ba-Cu-O compound^{47,48}. Although the actual mechanism of superconductivity in the cuprates is still under debate (and possibly not related to phonons dynamics), some researchers believe that the pairing could be mediated by (yet to be identified) bosonic excitations that live in the CuO layer^{49,50}.

Regardless of the ultimate nature of the bosonic “glue” at work in the cuprates, the fundamental point, for our purposes, is that due to strong interactions/correlations both the bosonic and fermionic quasiparticles are destroyed and no sharp peaks are observed in scattering experiments. Definitive proofs of this mechanism are the violation of the Mott-Ioffe-Regel (MIR) criterion which is experimentally observed at large temperatures⁵¹ and the anomalous thermal diffusion supported by recent studies^{52,53}.

The positive pressure effect on T_c observed in high- T_c cuprates could thus be explained within our proposed framework, as due to highly energetic but not quasiparticle-like bosonic excitations in the “incoherent” regime of our Fig.2. As a consistency check, the positive correlation of T_c with pressure has been indeed observed in the *underdoped* cuprates $\text{Bi}_2\text{Sr}_2\text{CuO}_{6+\delta}$ (Bi2201), which supports the theoretical framework presented above. Instead, in the *overdoped* cuprates $\text{Bi}_2\text{Sr}_2\text{CaCu}_2\text{O}_{8+\delta}$ (Bi2212) the dependence of T_c on P displays a minimum, just like in Fig.5, which suggests that the overdoped materials belong to the “coherent” regime.

This analysis thus provides a rationale for tuning the pressure effect on T_c in the cuprates via the oxygen doping, by explaining the positive correlation in the underdoped materials with the breakdown of the quasiparticle picture for the bosonic “glue”.

Conclusions

We presented a comprehensive theory of the pressure effect on Cooper pairing in superconductors where the pairing is mediated by generic bosonic excitations. Our theory is based on solving the gap equation with a bosonic propagator. A specific calculation is presented for optical phonons which takes into account: (i) the anharmonicity of the phonon via the Klemens’ damping, (ii) the effect of pressure on the phonon frequency.

The predictions of this theory are rich and far-reaching. First of all, the theory identifies two fundamental regimes as a function of the dimensionless ratio D between anharmonic phonon damping and phonon frequency. At low values of this ratio, T_c is strongly enhanced by anharmonicity and at the same decreases with increasing pressure. At large values of the D ratio (after a maximum), where the phonons are no longer well-defined quasiparticles, T_c instead correlates positively with pressure and is lowered by anharmonicity (see Fig. 2).

In the more conventional case of systems in the “coherent phonon” regime, where phonons are coherent quasiparticles, the standard linearly decreasing correlation between T_c and P is recovered using the Klemens theory of anharmonic damping for optical phonons. The theory, however, is able to describe also more complex materials. In particular, it provides a qualitative description of recent experimental data on TIInTe_2 for which phonon frequencies, anharmonic phonon damping and T_c were all measured experimentally. The theory predicts that T_c initially decreases with P as a consequence of the optical phonon energy increasing with P , but then goes through a minimum, as the optical phonon starts to soften and to become more anharmonic, after which it rises with P . The predicted behaviour is well supported by the experimental data.

This theoretical picture provides a comprehensive mechanistic rationale for the pressure effect on superconductivity, by physically describing different regimes of negative/positive pressure effect on T_c across a variety of materials, from simple elemental superconductors to complex unconventional materials. By clarifying the deep interplay between anharmonicity of the bosonic glue and pressure effects on the pairing mechanism, the theory provides new guidelines for material design, which may prove useful for discovering and/or engineering new materials with enhanced T_c .

Acknowledgements

M.B. acknowledges the support of the Spanish MINECO’s “Centro de Excelencia Severo Ochoa” Programme under grant SEV-2012-0249. C.S. is supported by the U.S. DOE grant number DE-FG02-05ER46236. A.Z. acknowledges financial support from US Army Research Laboratory and US Army Research Office through contract nr. W911NF-19-2-0055.

Author contributions

The first two authors, C.S. and M.B., contributed equally to this work. C.S., M.B. and A.Z. designed research, C.S. developed the analytical calculations and code with inputs from M.B. and A.Z., M.B. developed the graphics, A.Z. wrote the paper with inputs from C.S. and M.B.

References

1. Drozdov, A. P., Eremets, M. I., Troyan, I. A., Ksenofontov, V. & Shylin, S. I. Conventional superconductivity at 203 kelvin at high pressures in the sulfur hydride system. *Nature* **525**, 73–76, DOI: [10.1038/nature14964](https://doi.org/10.1038/nature14964) (2015).
2. Quan, Y., Ghosh, S. S. & Pickett, W. E. Compressed hydrides as metallic hydrogen superconductors. *Phys. Rev. B* **100**, 184505, DOI: [10.1103/PhysRevB.100.184505](https://doi.org/10.1103/PhysRevB.100.184505) (2019).
3. Drozdov, A. *et al.* Superconductivity at 250 k in lanthanum hydride under high pressures. *Nature* **569**, 528–531 (2019).
4. Pickard, C. J., Errea, I. & Eremets, M. I. Superconducting hydrides under pressure. *Annu. Rev. Condens. Matter Phys.* **11**, 57–76, DOI: [10.1146/annurev-conmatphys-031218-013413](https://doi.org/10.1146/annurev-conmatphys-031218-013413) (2020). <https://doi.org/10.1146/annurev-conmatphys-031218-013413>.
5. Trofimov, P. & Carbotte, J. Effect of pressure on superconductivity. *Solid State Commun.* **7**, 661 – 664, DOI: [https://doi.org/10.1016/0038-1098\(69\)90587-0](https://doi.org/10.1016/0038-1098(69)90587-0) (1969).
6. Trofimov, P. N. & Carbotte, J. P. Strong-coupling effects in the pressure dependence of superconductivity. *Phys. Rev. B* **1**, 1136–1143, DOI: [10.1103/PhysRevB.1.1136](https://doi.org/10.1103/PhysRevB.1.1136) (1970).

7. N.V. Zavaritskii, A. V., E.S. Itskevich. Effect of pressure on lattice oscillations and electron phonon interaction in superconductors. *Sov. Phys. JETP* **60**, 1408–1417 (1971).
8. Hodder, R. E. Pressure effects on the superconducting transition temperature of Pb. *Phys. Rev.* **180**, 530–534, DOI: [10.1103/PhysRev.180.530](https://doi.org/10.1103/PhysRev.180.530) (1969).
9. Brandt, N. B. & Ginzburg, N. I. SUPERCONDUCTIVITY AT HIGH PRESSURES. *Sov. Phys. Uspekhi* **12**, 344–358, DOI: [10.1070/pu1969v012n03abeh003900](https://doi.org/10.1070/pu1969v012n03abeh003900) (1969).
10. Bergmann, G. & Rainer, D. The sensitivity of the transition temperature to changes in $\alpha 2f(\omega)$. *Zeitschrift für Physik* **263**, 59–68 (1973).
11. Ashcroft, N. W. Metallic hydrogen: A high-temperature superconductor? *Phys. Rev. Lett.* **21**, 1748–1749, DOI: [10.1103/PhysRevLett.21.1748](https://doi.org/10.1103/PhysRevLett.21.1748) (1968).
12. Gardner, W. E. & Smith, T. F. Superconductivity of α -uranium and uranium compounds at high pressure. *Phys. Rev.* **154**, 309–315, DOI: [10.1103/PhysRev.154.309](https://doi.org/10.1103/PhysRev.154.309) (1967).
13. Prakash, O., Kumar, A., Thamizhavel, A. & Ramakrishnan, S. Evidence for bulk superconductivity in pure bismuth single crystals at ambient pressure. *Science* **355**, 52–55, DOI: [10.1126/science.aaf8227](https://doi.org/10.1126/science.aaf8227) (2017). <https://science.sciencemag.org/content/355/6320/52.full.pdf>.
14. Behnia, K. The fragility of distant cooper pairs. *Science* **355**, 26–27, DOI: [10.1126/science.aal2516](https://doi.org/10.1126/science.aal2516) (2017).
15. Wittig, J. Die supraleitung von zinn und blei unter sehr hohem druck. *Zeitschrift für Physik* **195**, 228–238, DOI: [10.1007/BF01328890](https://doi.org/10.1007/BF01328890) (1966).
16. Baggiooli, M., Setty, C. & Zaccone, A. Effective theory of superconductivity in strongly coupled amorphous materials. *Phys. Rev. B* **101**, 214502, DOI: [10.1103/PhysRevB.101.214502](https://doi.org/10.1103/PhysRevB.101.214502) (2020).
17. Lorenz, B. & Chu, C. *High Pressure Effects on Superconductivity*, 459–497 (Springer Berlin Heidelberg, Berlin, Heidelberg, 2005).
18. Errea, I. *et al.* High-pressure hydrogen sulfide from first principles: A strongly anharmonic phonon-mediated superconductor. *Phys. Rev. Lett.* **114**, 157004 (2015).
19. Rousseau, B. & Bergara, A. Giant anharmonicity suppresses superconductivity in alh 3 under pressure. *Phys. Rev. B* **82**, 104504 (2010).
20. Errea, I., Calandra, M. & Mauri, F. First-principles theory of anharmonicity and the inverse isotope effect in superconducting palladium-hydride compounds. *Phys. Rev. Lett.* **111**, 177002, DOI: [10.1103/PhysRevLett.111.177002](https://doi.org/10.1103/PhysRevLett.111.177002) (2013).
21. Errea, I., Calandra, M. & Mauri, F. Anharmonic free energies and phonon dispersions from the stochastic self-consistent harmonic approximation: Application to platinum and palladium hydrides. *Phys. Rev. B* **89**, 064302, DOI: [10.1103/PhysRevB.89.064302](https://doi.org/10.1103/PhysRevB.89.064302) (2014).
22. Errea, I. *et al.* Quantum hydrogen-bond symmetrization in the superconducting hydrogen sulfide system. *Nature* **532**, 81–84 (2016).
23. Sano, W., Koretsune, T., Tadano, T., Akashi, R. & Arita, R. Effect of van hove singularities on high- T_c superconductivity in h_3S . *Phys. Rev. B* **93**, 094525, DOI: [10.1103/PhysRevB.93.094525](https://doi.org/10.1103/PhysRevB.93.094525) (2016).
24. Borinaga, M. *et al.* Anharmonic enhancement of superconductivity in metallic molecular cmca- 4 hydrogen at high pressure: a first-principles study. *J. Physics: Condens. Matter* **28**, 494001 (2016).
25. Borinaga, M., Errea, I., Calandra, M., Mauri, F. & Bergara, A. Anharmonic effects in atomic hydrogen: Superconductivity and lattice dynamical stability. *Phys. Rev. B* **93**, 174308, DOI: [10.1103/PhysRevB.93.174308](https://doi.org/10.1103/PhysRevB.93.174308) (2016).
26. Szczęśniak, D. & Zemła, T. On the high-pressure superconducting phase in platinum hydride. *Supercond. Sci. Technol.* **28**, 085018 (2015).
27. Kostrzewska, M., Szczęśniak, K., Durajski, A. & Szczęśniak, R. From lah 10 to room-temperature superconductors. *Sci. Reports* **10**, 1–8 (2020).
28. Errea, I. *et al.* Quantum crystal structure in the 250-kelvin superconducting lanthanum hydride. *Nature* **578**, 66–69 (2020).
29. Camargo-Martínez, J. A., González-Pedreros, G. I. & Mesa, F. The higher superconducting transition temperature t_c and the functional derivative of t_c with $\alpha^2 f(\omega)$ for electron-phonon superconductors (2020). [2006.15248](https://doi.org/10.4236/ojs.20200615248).
30. Klemens, P. Anharmonic decay of optical phonons. *Phys. Rev.* **148**, 845 (1966).

31. Yesudhas, S. *et al.* Origin of superconductivity and giant phonon softening in TIInTe_2 under pressure. *arXiv preprint arXiv:2003.09804* (2020).
32. Kunc, K., Loa, I. & Syassen, K. Equation of state and phonon frequency calculations of diamond at high pressures. *Phys. Rev. B* **68**, 094107, DOI: [10.1103/PhysRevB.68.094107](https://doi.org/10.1103/PhysRevB.68.094107) (2003).
33. Birch, F. Finite elastic strain of cubic crystals. *Phys. Rev.* **71**, 809–824, DOI: [10.1103/PhysRev.71.809](https://doi.org/10.1103/PhysRev.71.809) (1947).
34. Allen, P. B., Feldman, J. L., Fabian, J. & Wooten, F. Diffusons, locons and propagons: Character of atomic vibrations in amorphous si. *Philos. Mag. B* **79**, 1715–1731, DOI: [10.1080/13642819908223054](https://doi.org/10.1080/13642819908223054) (1999). <https://doi.org/10.1080/13642819908223054>.
35. Marsiglio, F. & Carbotte, J. Electron-phonon superconductivity. In *Superconductivity*, 73–162 (Springer, 2008).
36. Kleinert, H. *Collective classical and quantum fields* (World Scientific, Singapore, 2018).
37. Ioffe, A. & Regel, A. Non-crystalline, amorphous and liquid electronic semiconductors. *Prog. Semicond* **4**, 237–291 (1960).
38. Krivtsov, A. M. & Kuz'kin, V. A. Derivation of equations of state for ideal crystals of simple structure. *Mech. Solids* **46**, 387, DOI: [10.3103/S002565441103006X](https://doi.org/10.3103/S002565441103006X) (2011).
39. Cuffari, D. & Bongiorno, A. Calculation of mode grüneisen parameters made simple. *Phys. Rev. Lett.* **124**, 215501, DOI: [10.1103/PhysRevLett.124.215501](https://doi.org/10.1103/PhysRevLett.124.215501) (2020).
40. Boughton, R., Olsen, J. & Palmy, C. Chapter 4 pressure effects in superconductors. vol. 6 of *Progress in Low Temperature Physics*, 163 – 203, DOI: [https://doi.org/10.1016/S0079-6417\(08\)60063-3](https://doi.org/10.1016/S0079-6417(08)60063-3) (Elsevier, 1970).
41. Setty, C. Glass-induced enhancement of superconducting T_c : Pairing via dissipative mediators. *Phys. Rev. B* **99**, 144523, DOI: [10.1103/PhysRevB.99.144523](https://doi.org/10.1103/PhysRevB.99.144523) (2019).
42. Setty, C., Baggiooli, M. & Zacccone, A. Phonon anharmonicity enhances the t_c of bcs-type superconductors. *arXiv preprint arXiv:2003.06220* (2020).
43. Manley, M. E. *et al.* Large harmonic softening of the phonon density of states of uranium. *Phys. Rev. Lett.* **86**, 3076–3079, DOI: [10.1103/PhysRevLett.86.3076](https://doi.org/10.1103/PhysRevLett.86.3076) (2001).
44. Baggiooli, M. & Zacccone, A. Universal origin of boson peak vibrational anomalies in ordered crystals and in amorphous materials. *Phys. Rev. Lett.* **122**, 145501, DOI: [10.1103/PhysRevLett.122.145501](https://doi.org/10.1103/PhysRevLett.122.145501) (2019).
45. Riseborough, P. S. & Yang, X. Phonon anomalies in α -uranium. *J. Magn. Magn. Mater.* **310**, 938 – 940, DOI: <https://doi.org/10.1016/j.jmmm.2006.10.215> (2007). Proceedings of the 17th International Conference on Magnetism.
46. Fietz, W. *et al.* Giant pressure effect in oxygen deficient $\text{yba}_2\text{cu}_3\text{ox}$. *Phys. C: Supercond.* **270**, 258 – 266, DOI: [https://doi.org/10.1016/S0921-4534\(96\)00480-7](https://doi.org/10.1016/S0921-4534(96)00480-7) (1996).
47. Chu, C. W. *et al.* Evidence for superconductivity above 40 k in the la-ba-cu-o compound system. *Phys. Rev. Lett.* **58**, 405–407, DOI: [10.1103/PhysRevLett.58.405](https://doi.org/10.1103/PhysRevLett.58.405) (1987).
48. CHU, C. W., HOR, P. H., MENG, R. L., GAO, L. & HUANG, Z. J. Superconductivity at 52.5 k in the lanthanum-barium-copper-oxide system. *Science* **235**, 567–569, DOI: [10.1126/science.235.4788.567](https://doi.org/10.1126/science.235.4788.567) (1987). <https://science.sciencemag.org/content/235/4788/567.full.pdf>.
49. Dagotto, E. Correlated electrons in high-temperature superconductors. *Rev. Mod. Phys.* **66**, 763–840, DOI: [10.1103/RevModPhys.66.763](https://doi.org/10.1103/RevModPhys.66.763) (1994).
50. Lee, P. A., Nagaosa, N. & Wen, X.-G. Doping a mott insulator: Physics of high-temperature superconductivity. *Rev. Mod. Phys.* **78**, 17–85, DOI: [10.1103/RevModPhys.78.17](https://doi.org/10.1103/RevModPhys.78.17) (2006).
51. Zhang, J. *et al.* Thermal diffusivity above the mott-ioffe-regel limit. *Phys. Rev. B* **100**, 241114, DOI: [10.1103/PhysRevB.100.241114](https://doi.org/10.1103/PhysRevB.100.241114) (2019).
52. Zhang, J. *et al.* Anomalous thermal diffusivity in underdoped $\text{yba}_2\text{cu}_3\text{o}_6+\text{x}$. *Proc. Natl. Acad. Sci.* **114**, 5378–5383, DOI: [10.1073/pnas.1703416114](https://doi.org/10.1073/pnas.1703416114) (2017). <https://www.pnas.org/content/114/21/5378.full.pdf>.
53. Zhang, J. *et al.* Thermal diffusivity above the mott-ioffe-regel limit. *Phys. Rev. B* **100**, 241114, DOI: [10.1103/PhysRevB.100.241114](https://doi.org/10.1103/PhysRevB.100.241114) (2019).